MODULATION OF THE ENDOTHELIAL PHENOTYPE BY TRANSFORMING GROWTH FACTOR-β2 AND NCK SIGNALING

An Undergraduate Research Scholars Thesis

by

THAO-NGUYEN PHAM

Submitted to the Undergraduate Research Scholars program at
Texas A&M University
in partial fulfillment of the requirements for the designation as an

UNDERGRADUATE RESEARCH SCHOLAR

Approved by Research Advisor: Dr. Gonzalo Rivera

May 2019

Major: Zoology
Wildlife and Fisheries

TABLE OF CONTENTS

ABSTRACT

Modulation of the Endothelial Phenotype by Transitional Growth Factor-β2 and Nck Signaling

Thao-Nguyen Pham
Department of Biology
Department of Wildlife and Fisheries Science
Texas A&M University

Research Advisor: Dr. Gonzalo Rivera
Department of Veterinary Pathobiology
Texas A&M University

The development of solid tumors requires neovascularization. In contrast to blood vessels of healthy organs, blood vessels associated with atherosclerosis and tumors are poorly organized and leaky. However, it is poorly understood how microenvironmental factors modulate molecular mechanisms underlying the abnormal vascular phenotype. The objective in this project is to determine cellular changes elicited by transforming growth factor-β2 (TGF-β2) and the Nck adaptors in the transition of endothelial sheets from a stable/cohesive to a loosely organized, permeable phenotype. It is hypothesized that the Nck adaptors link heightened matrix stiffness and TGF-β2 signaling thereby inducing cytoskeletal changes underlying the tumor-associated endothelial phenotype. Cell culture experiments coupled with immunofluorescence labeling indicate change in cell morphology and patterns of protein expression/subcellular distribution when TGF-β2-treated cells were compared with control endothelial cells. Preliminary results indicate the Nck modulates TGF-beta-induced changes in cell morphology. These results suggest that the TGF-β2 signaling pathway and/or the silencing of the Nck could be targeted to prevent Endothelial to Mesenchymal Transition (EndMT) and the abnormal vasculature in atherosclerosis.

ACKNOWLEDGEMENTS

I would like to first and foremost express my deepest appreciation to my research professor, Dr. Gonzalo Rivera, for giving me the opportunity to join the research team. Your constructive suggestions and encouragement throughout the planning and experimentation steps helped me build self-confidence, be creative, and have perseverance when my experiments fail.

I would also like to thank Briana Bywaters for taking me under her wing, giving me continuing mentorship and believing in my abilities. From day one, because you were relatable and patient, I felt excited to contribute my time and effort in this project, though I lacked experience. Your guidance has helped me gain the skills and knowledge to succeed in this research project over the past year, and I look forward to continue working with you.

I would also like to include a special note of thanks to my lab teammates, Tien Tran and Gladys Pedraza, for their contribution to this research project with data from western blotting and Nck and Cre effects in mice. The completion of this study could not have been possible without the expertise of the following people: Dr. Daniel Alge, Dr. Andreea Trache, Samantha Holt and Amanda Rakoshia for assisting me in understanding the protocol and sharing materials for the fabrication of the hydrogels. Special thanks to Dr. Rola Barhoumi Mouneimne (CVM Image Analysis Laboratory) for imaging the HUVEC cells for later analysis.

A deal of gratitude is also owed to the National Education Foundation, American Heart Association Foundation, TAMU T3 program, and the Veterinary Pathobiology Department for funding of this research.

Finally, I would like to thank my friends and family for their unparalleled support, for comforting me when I suffered setbacks and failures.

NOMENCLATURE

AHA	American Heart Association
EndMT	Endothelial Mesenchymal Transition
HUVEC	Human Umbilical Vein Endothelial Cells
PEG	Polyethylene glycol hydrogels
SM22-α	smooth muscle 22
TGF-β2	Transforming Growth Factor - Beta 2
VE-Cad	VE-Cadherin
VEGF	Vascular Endothelial Growth Factor

CHAPTER I

INTRODUCTION

Significance

The American Heart Association (AHA) states that atherosclerosis is one of the leading causes of vascular disease worldwide (Momiyama 2014). When the blood vessels narrow due to plaque formation in the artery wall, it increases blood pressure by forcing the heart to pump blood faster through the arteries due to the decreased diameter of the vessel walls. This increases the risk of a stroke or heart attack. At a cellular level, we hypothesize that plaque formation is promoted by endothelial cells transitioning into mesenchymal cells.

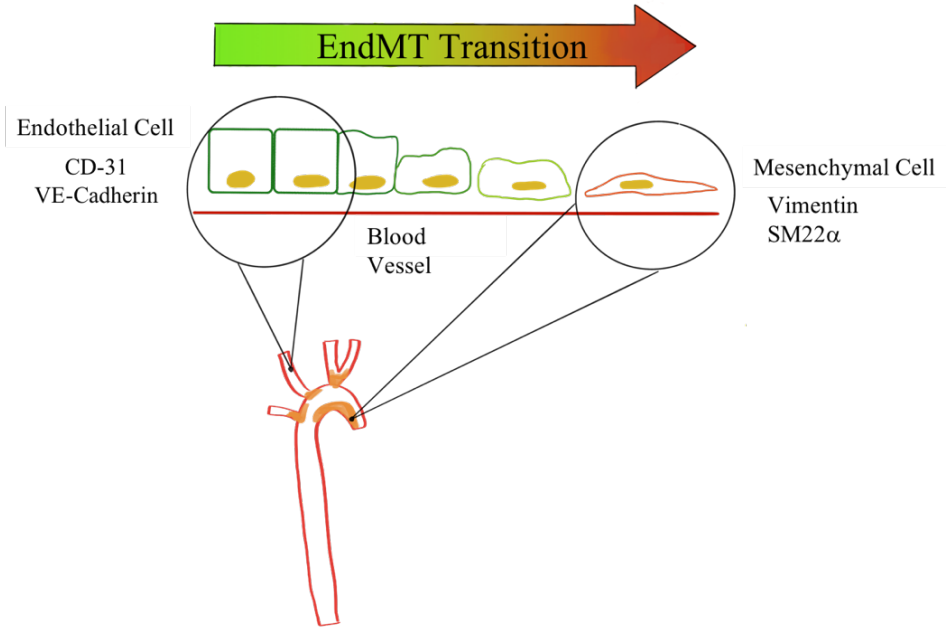

Figure 1. EndMT is linked to plaque development. As endothelial cells take on a mesenchymal phenotype, risk of plaque development increases.

Endothelial cells make up the lining of blood vessels, express apical-basal polarity, and have a cobblestone morphology as depicted in Figure 1. Their tight junctions and cell-to-cell

adhesions create a strong, yet permeable barrier. In contrast to the quiescent vasculature, endothelial cells experience phenotypic changes consistent with EndMT in vascular beds undergoing angiogenesis.

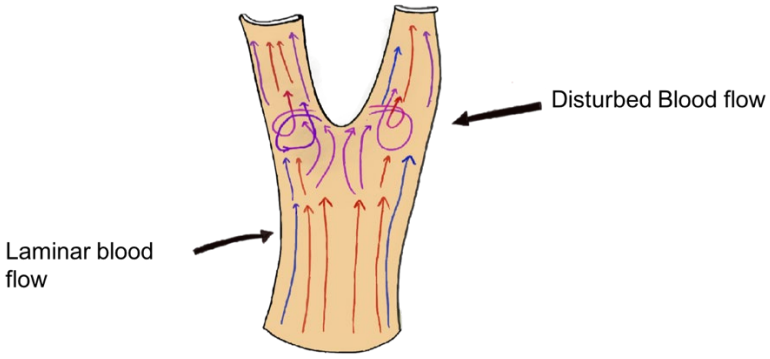

Figure 2. Aortic geometry affects blood flow patterns. Laminar blood flow is disturbed at bifurcations. Disturbed flow activates ECs which contributes to EndMT. Red denotes rapid flow, blue, slower flow, and purple, disturbed flow.

The earliest stage of atherosclerosis is intimal stiffening ((Miroshnikova et al., 2016). The stiffening of the matrix results in more TGF-β2 being released by the cells, eventually resulting in stiffer blood vessels, as demonstrated in the human carotid bifurcation in Figure 2. The blood flow in the outer region of the blood vessel is characterized as laminar flow, in contrast to the forked area where the vessel splits, where-in blood flow characterized as a disturbed flow (Miroshnikova et al., 2012). The topography of the forked area results in blood hitting the side of the vessel, creating a circular, turbulent flow which explains why some areas in the human aorta are more susceptible to atherosclerosis than others (Miroshnikova et al., 2012).

The abnormal tumor vasculature contributes to tumor progression and metastasis (Miroshnikova et al., 2012). The leaky nature of the vasculature in solid tumors results in increased interstitial pressure and thereby decreased diffusion of anticancer drugs. In addition,

the poor architectural organization of the tumor vasculature facilitates intravasation of invasive cancers cells and metastatic spread. Therapeutic strategies aimed at limiting the abnormal vascular growth in tumors, particularly targeting vascular endothelial growth factor (VEGF) signaling, have shown limited effectiveness. Unfortunately, the development of resistance to such therapies has been linked to tumor relapse and disease progression (Jung et. Al.,2017 ; Rigamonti et al., 2014). Thus, a better understanding of cellular and molecular mechanisms underlying tumor angiogenesis holds promise for the development of new and improve anti-cancer treatments.

Scientific Premise

Emerging evidence suggests that, under conditions prevalent in the tumor microenvironment, vascular endothelial sheets undergo a phenotypic switch from a stable/cohesive state to a mesenchymal-like state characterized by altered cell-cell junctional organization and increased permeability (Millan et al., 2010). Within the tumor microenvironment, matrix stiffening (Miroshnikova et al., 2016) and increased TGF-β2 signaling (Liu et al., 2012) are critical cues promoting a tumor vascular phenotype.

Approach

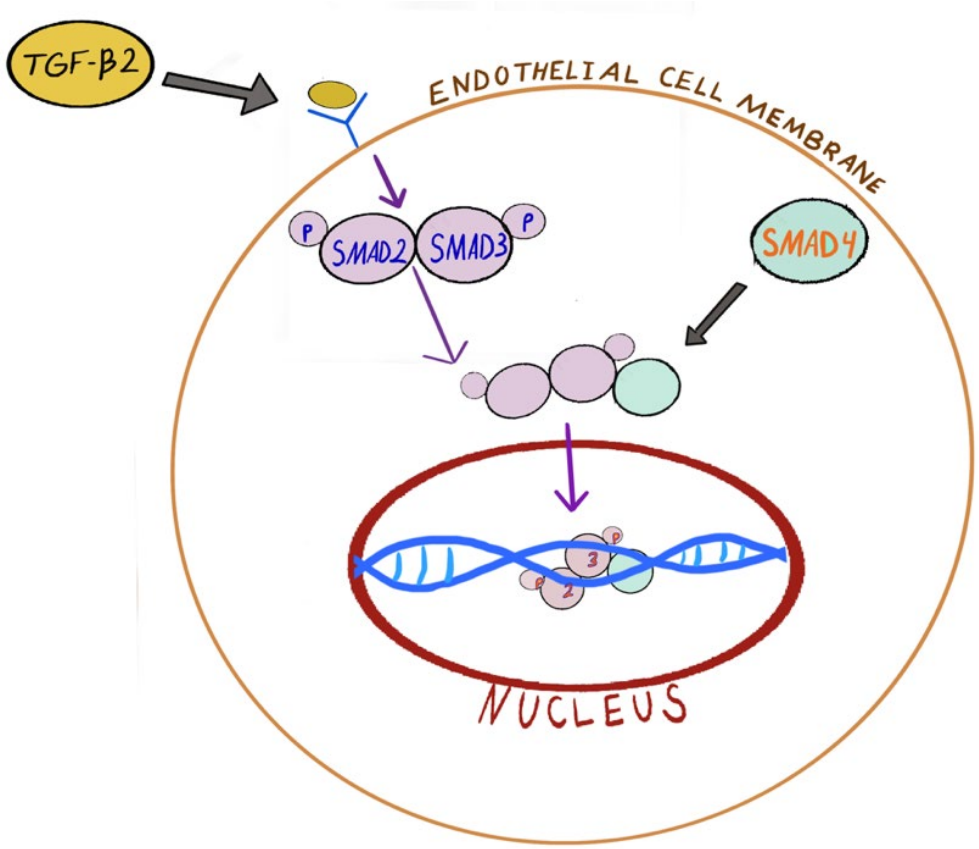

Figure 3. TGF-β2 activates the Smad pathway. Phosphorylated Smad 2 and 3 form a complex with Smad 4 in the cytosol and travel to the nucleus to alter gene transcription.

Figure 3 shows a diagram of TGF-β2 and its hypothesized effect. TGF-β2, the primary signal molecule for EndMT, phosphorylates SMAD 2 and 3. The SMAD forms a heterotrimeric complex with SMAD 4, and travel from cytosol to nucleus, where they alter gene expression (Cooley et al., 2014). This results in a down-regulation of endothelial genes, and an upregulation of mesenchymal genes, which via transcription and translation produce proteins that with immunofluorescent staining and confocal imaging can be observed and quantified (Chen et al., 2015a).

One main consequence of EndMT is altered integrity of the endothelial barrier as a result of partial disassembly of cell-to-cell adhesions. The intensity and distribution of the VE-Cadherin (VE-Cad) marker will be measured to quantify the effect of TGF-β2 (Erasmus et al., 2016). The decrease in VE-Cad in cells treated with TGF-β2 is expected. Furthermore, the decrease in the endothelial marker CD31 at the junctions between cells will denote EndMT. The two mesenchymal markers, Vimentin and SM22-α, are both expected to have an upregulation in cells treated with TGF-β2. Vimentin is an intermediate filament and SM22-α is smooth muscle actin protein. The overall cytoskeleton organization will be assessed by labeling F-actin (Erasmus et al., 2016).

Research Design

To monitor and detect EndMT progression, we used immunofluorescence staining with specific antibodies for each endothelial and mesenchymal marker (Chen et al., 2015a). This will create a visual image of the HUVEC cells fixed after TGF-β2 induction, allowing the architectural integrity of the cell to be assessed overall (Baumgartner et al., 2003). Table 1, 2, and 3 denotes the general timeline of each experiment performed in these experiments.

CHAPTER II

METHODS

in vitro cell culturing

HUVEC cells were all frozen at passage 5 (P5) and were then thawed to room temperature. They were plated with either complete media or starvation media in a 10 cm fibronectin coated plate. Fresh media was added after 24 hours to remove any dead or unattached cells. Subsequently, fresh media was changed every other day until 50% confluence.

in vitro Induction of EndMT

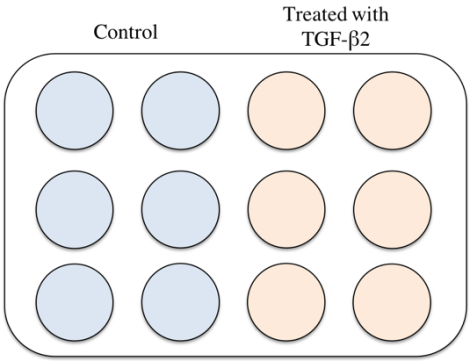

Figure 4. A representation of the 12-well plate used in Experiment 1 and Experiment 2.

At passage 6, the cells were seeded at a density of 7.5 x 10^4 cells/cm^2 onto a fibronectin coated coverslip placed inside each well of a 12-well plate as denoted in Figure 4. After 24 hours, half of the wells received either complete media or starve media with TGFβ-2 and the other half received only complete media or starve media (Table 1). The non-induced cells were used as the control.

Treatment with TGF-beta and washing steps of immunofluorescence were performed in the wells. Coverslips were removed during the blocking/IF steps and mounted on a microscope coverslip with Prolong Gold (Appendix A).

Table 1. Timeline overview of the protocol performed for Experiments 1-2

	Day 1	Day 2	Day 3	Day 4	Day 5	Day 6
Experiment 1	Plate cells onto 10 cm plate	Change complete media	Pass cells onto coverslips	Add TGF-β2 to half of the wells	Add TGF-β2 to half of the wells	Fix and probe
Experiment 2	Plate cells onto 10 cm	Change starve media	Pass cells onto coverslips	Add TGF-β2 to half of the wells	Add TGF-β2 to half of the wells	Fix and Probe

Note: Antibodies probed are listed in the methods, Appendix A, and are discussed in the results

siRNA and siNck-mediated silencing

HUVEC cells at P5 and P3 were cultured on 10 cm plates, then at 90% confluence cells were passed into fibronectin-coated 6-well plates with a plating density of 20 x 10^4cells/cm^2. After 24 hours, the complete media was changed to antibiotic free serum in preparation for the transfection procedure.

Table 2. Dilutions preparation of siRNA with antibiotic-free complete media.

Plating Format	Surface Area (cm^2/well)	Tube 1: diluted siRNA (µl/well)		Tube 2: diluted DharmaFECT (µl/well)	
		Volume of 5uM siRNA (µl)	Serum-free Medium (µl)	Volume of DharamaFECT4 reagent (µl)	Basal Medium (µl)
6-well plate siNck	10	Nck1: 10 Nck2: 10	160	4	196
6-well plate siScr	10	10	190	4	196

The transfection method was modified from previous research (Pils et al., 2012). Dilutions of siRNA with basal media were prepared by combining diluted siRNA media with diluted DharmaFECT (Table 2).

Table 3. Timeline of protocols performed for transfection followed by TGF-β treatment.

Day 1	Day 2	Day 3	Day 4	Day 5	Day 6	Day 7	Day 8
Plate cells onto 10cm plate	Change media (CM)	Pass onto 6-well plates	siRNA; siNck knockdown	Pass onto coverslips in 12-well plate	Add TGF-β2 to half of wells	Add TGF-β2 to half of wells	Fix and IF cells

After the mixtures were added accordingly to each well, cells were incubated at 37°C for 6 hours before the antibiotic-free media was replaced with complete media (Table 3).

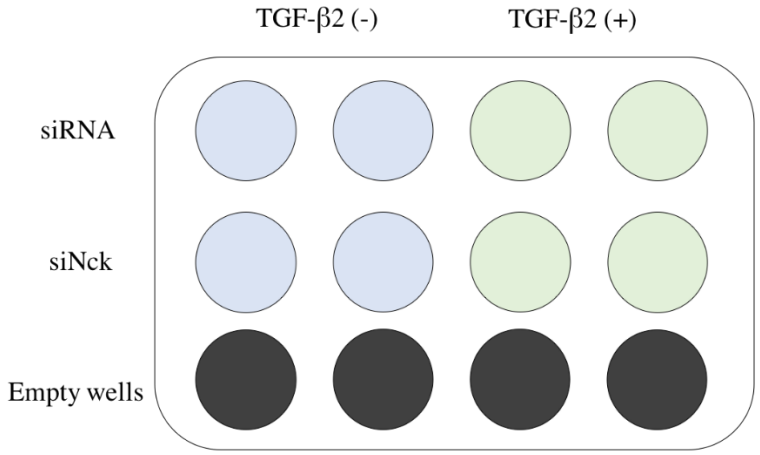

Figure 5. 12-well plate for Day 5 and Day 6 TGF-β2 treatment. 8 out of 12 wells were used in each plate. One plate was used each for VE-Cad and vimentin.

After 24 hours of incubation with complete media, cells were collected on Day 5 and passed at 7.5 x 10^4cells/cm^2 to 16 total fibronectin coated coverslips followed by 24 and 48 hour TGF-β2 treatments of siNck1, siNck 2, and siScr (Table 3, Figure 5, Appendix A).

Immunofluorescence

The immunofluorescence protocol was modified from previous research (Erasmus et al., 2016) with different antibodies used for this study. At passage 7, 4% paraformaldehyde was used to fix the cells, followed by blocking in complete buffer (CB) and 2% Bovine Serum Albumin (BSA) (Appendix A).

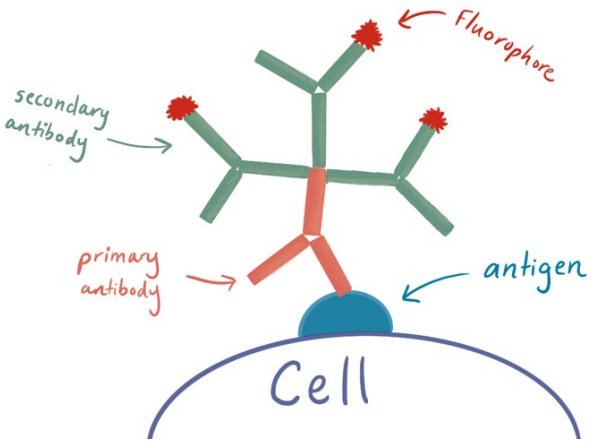

Figure 6. Indirect immunofluorescence allows visualization of specific proteins. Primary antibodies bind specific proteins. Fluorescently labeled secondary antibodies bind to the primary based on species.

The antibodies were incubated at room temperature for an hour with the following antibodies: VE-Cad (1:500, sc-9989), vimentin (1:500, sc-6260), f-actin phalloidin (1:200, REF T7471) and SM22α (1:500, ab14106) (Figure 6). Then was then followed by the secondary antibody blocking, at room temperature, with goat-anti mouse Alexa Fluor 488 (REF A11034) and goat-anti rabbit Alexa Fluor 647 (REF A11029)(Figure 6) (Appendix A). Prolong Gold was used to adhere the coverslip to a microscope slide. After 24 hours of storage in darkness, the mounted cells were imaged with a LSM780 confocal microscope at different wavelengths and planes. The images were later analyzed with ImageJ.

Fabrication of Hydrogels

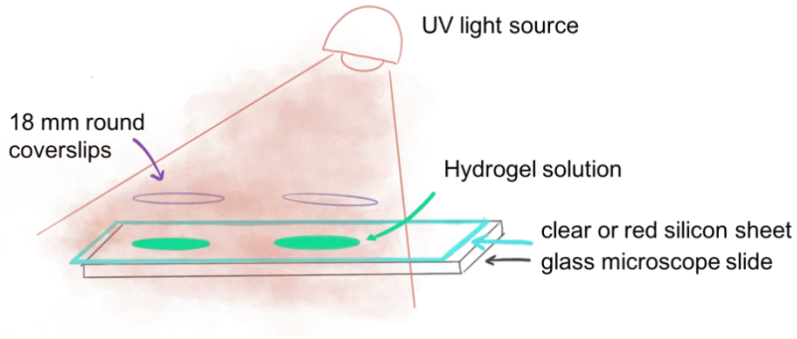

Figure 7. Fabrication of PEG-based hydrogels. Stiff (23 kPa) and soft (4.5 kPa) hydrogels are cured on 18 mm round coverslips using a UV mediated light source for 5 minutes.

Future experiments will test how the synergism between matrix stiffness and TGF-β modulates the phenotype of HUVECs. Polyethylene glycol hydrogels (PEG) coated with fibronectin to resemble the tumor microenvironment were designed with stiffness of normal tissue (~4.5 kPa) or tumor tissue (23 kPa) (Figure 7, Figure 8). The overall stiffness of the hydrogels increased with a decrease in mesh size and increase in concentration of the PEG-compounds.

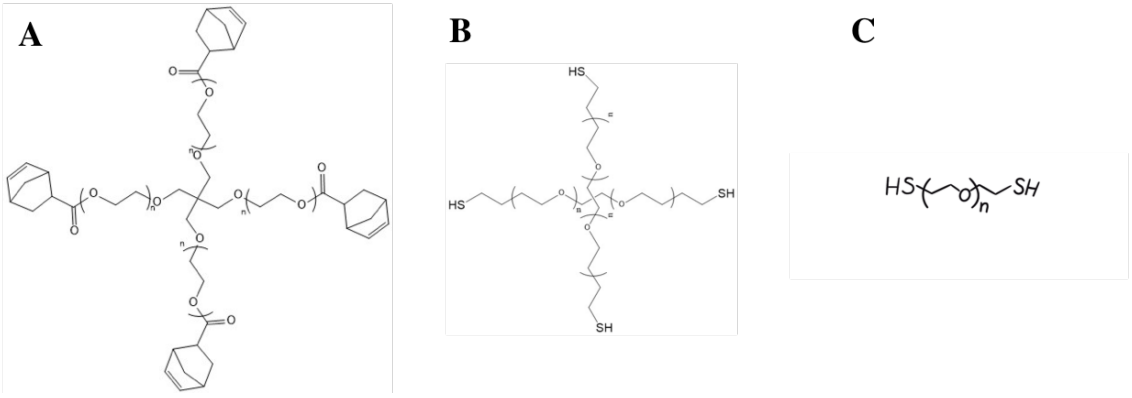

Figure 8. Hydrogel composition. Both stiff and soft gels were made with 4-arm-PEG-norbornene. **B.** For stiffer gels, 4-arm-PEG-tetra-thiol was added. **C.** For softer gels, PEG di-thiol was added.

Endothelial cells plated on stiff and soft hydrogels will be left untreated (control) or treated with TGF-β2 at 24 hours and 48 hours. If results indicate significant morphological changes, deletion of the Nck gene and TGF-β2 treatment will also be tested to confirm the role of Nck in EndMT.

CHAPTER III

RESULTS

TGF-β2 induction of EndMT in HUVEC cells

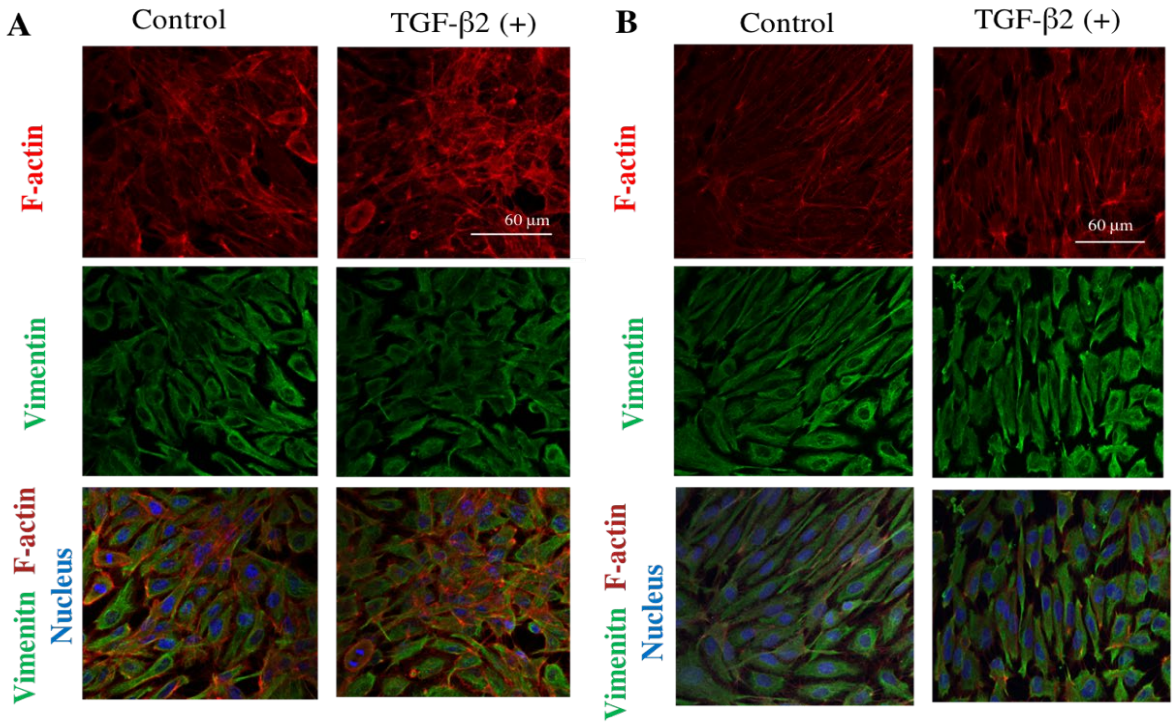

Figure 9. A and B *in vitro* immunostaining for endothelial and mesenchymal markers in HUVEC cells. Scale bar denotes 60 µm. In TGFβ-2 treated cultures, induction of EndMT is denoted from an upregulation of f-actin (phalloidin) stress fibers and a less cobblestone-like morphology. **A.** Experiment 1: cells were cultured in complete media and (right) TGF-β2 (10ng/mL). **B.** Experiment 2: cells were cultured in starve media (0.2% serum) and (right) TGF-β2 (10ng/mL).

TGF-β2 is one of the established pathways that regulates EndMT (Cooley et al., 2014). F-actin, measured with phalloidin (red, Figure 9A), appeared the same in distribution and intensity

in both control and TGF-β2 treated. However, the use of starvation media with TGF-β2 remodeled the actin cytoskeleton matrix (Figure 9B). The increase in actin fibers was expected once the cells were induced with TGF-β2 and incubated in starve media. The increased expression of EndMT could also be from the addition of stress fibers, since the amount of stress fibers directly correlates to the stiffness of the cell. Further stiffening of the cell is another morphological change in EndMT (Liu et al., 2012).

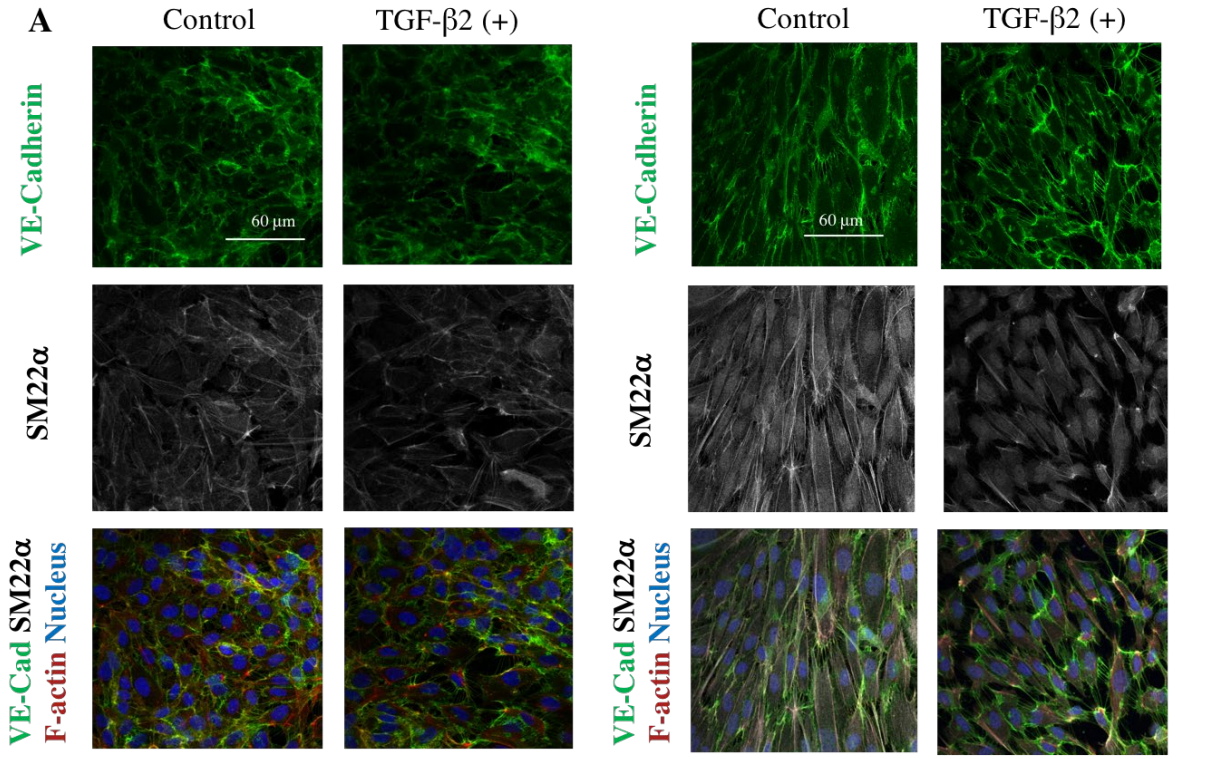

Fig

Figure 10A and B. *in vitro* immunostaining for endothelial and mesenchymal markers in HUVEC cells. Scale bar denotes 60 µm. In TGFβ-2 treated cultures, induction of EndMT is denoted from an upregulation of SM22-α. VE-Cadherin intensity is reduced, indicated by thinner adhesions. **A.** Experiment 1: cells were cultured in complete media and (right) TGF-β2 (10ng/mL). **B.** Experiment 2: cells were cultured in starve media (0.2% serum) and (right) TGF-β2 (10 ng/mL).

There was a deregulation of VE-Cadherin in TGF-β2-treated HUVEC cells in both Figures 10A and 10B. The VE-Cad marker is distributed more in the cytoplasm of TGF-β2 treated cells compared to the extracellular location in control cells. Overall, there are also thinner filaments in the TGF-β2 treated cells. Both indicate a disruption of endothelial cell-to-cell junctions, as endothelial cells lose their cobblestone-like shape and transition into narrow fibroblast shaped cells, consistent with a migratory phenotype.

The amount of vimentin was not noticeable difference between control and TGF-β2 treated cells cultured in complete media (Figure 9A) or starve media (Figure 9B). This might be due to the homogenous stiffness from the coverslips. Further examination of the vimentin marker could be performed on soft and stiff hydrogels to compare the amount of intermediate mesenchymal filaments. SM22-α, a mesenchymal marker, is expected to show an upregulation in TGF-β2 induced cells. The results indicate there was no upregulation in SM22-α, when cultured in complete media. However, cells cultured in starve media show an is an increase in intensity of SM22-α, located on the stress fibers.

A

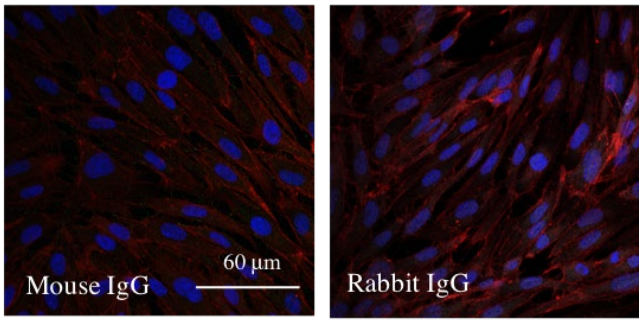

Fig 11A. Immunostaining of *in vitro* HUVEC cells and EndMT markers, with the nucleus stained blue. Scale bar denotes 60 µm. Both IgG mouse and IgG rabbit antibodies were used as isotype control.

The signals in the cytoplasm appear to be background noises as denoted in Figure 11A with IgG rabbit antibody. The overall change in the appearance of the cells is an indicator of EndMT. The cells start to lose their cobblestone-like shape and transform into spindle-shaped, fibroblast-like shape when induced by TGF-β2. The endothelial phenotype is affected by the TGF-β2 pathway as endothelial markers are gradually decreasing when mesenchymal markers are increasing. The switch from the stable/cohesive phenotype to a tumor-like state reflects previous research (Millan et al., 2010).

Effect of silencing Nck adaptor proteins and TGF-β2 treatment

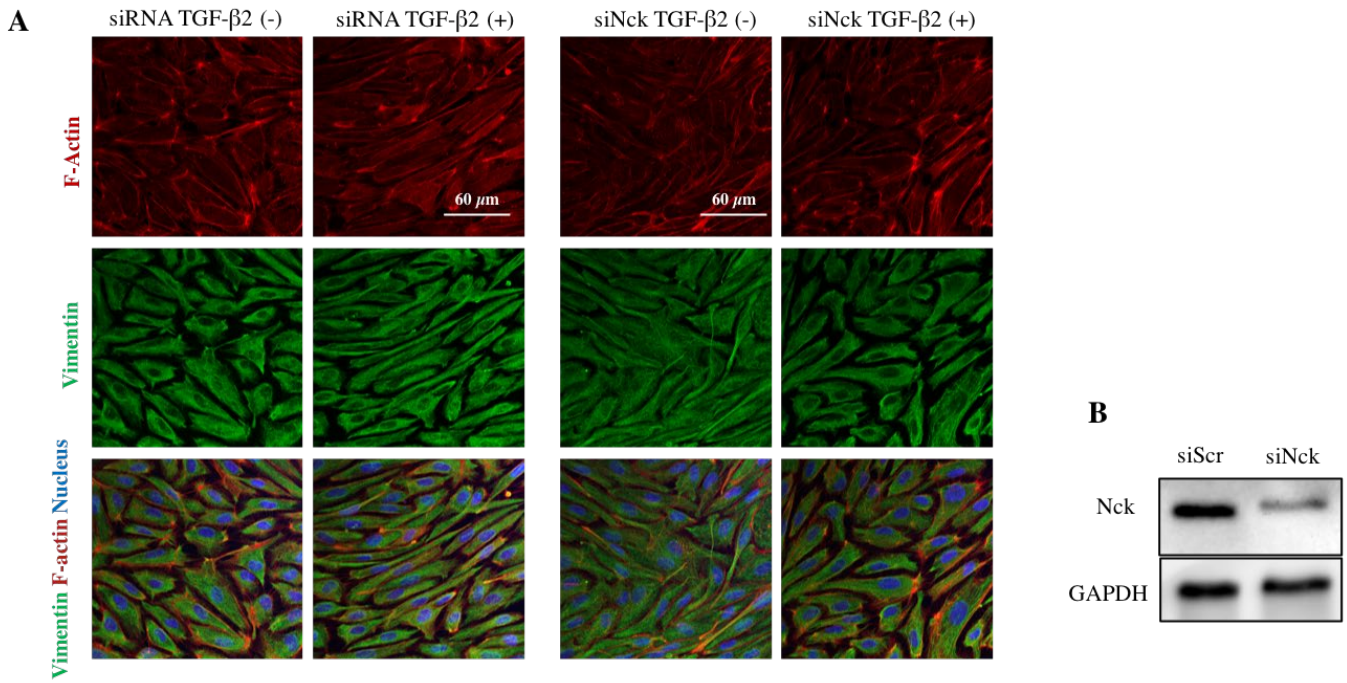

Figure 12) A. Nck deletion affects cell morphology. **B. Analysis of Western Blots.** Results indicate a reduction in the amount of siNck protein present after the transfection procedure.

To serve as a baseline, experimentation was performed several times to determine that TGF-β2 induced EndMT in this lab. Overall, the group of cells treated with TGF-β2 appear to be more elongated, a sign of endothelial to mesenchymal transition (Figure 12). The Western Blot

results indicate that there was an equal loading of GAPDH, siRNA, and siNck. The decrease in Nck protein indicates the transfection procedure successfully knocked down the Nck gene in the HUVECs (Figure 12B). The immunostaining results visually parallel the Western Blot results with the differing intensity of vimentin and f-actin (Figure 12A). Between the control and siNck group, the cells in the control group have a more specific intensity of F-actin at the cellular membrane (Figure 12).

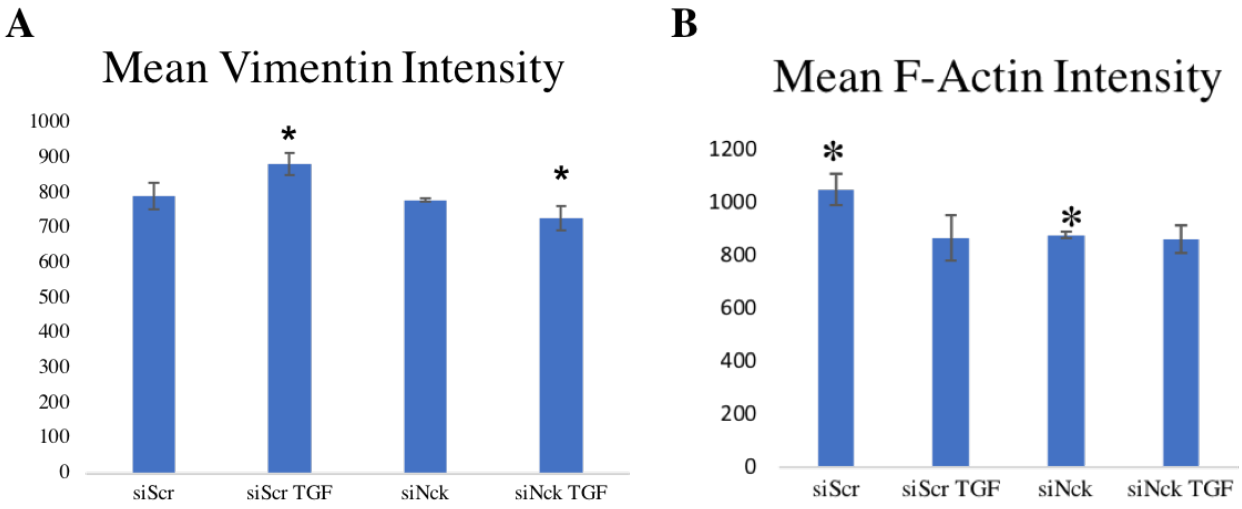

Figure 13A. Nck deletion attenuates vimentin upregulation. B. Nck deletion lowers F-Actin levels.

Presented in Figure 12, the intensity of fibers expressed is highest in control cells treated with TGF-β2, indicating that knocking down the Nck genes alter cytoskeleton formation while silencing RNA did not interfere with cellular function. Based on preliminary findings, deletion of Nck in HUVECs alters their phenotype and morphology, suggesting that Nck plays a role in the connection between TGF-β2 and the production of stress fibers.

Between control and Nck-silenced cells, there is a higher concentration of vimentin clustered closer to the nucleus in the former than latter (Figure 13). This contrasts with the Nck-

silenced group, where vimentin appears to be clustered closer to the plasma membrane. These results may indicate that cells in the control group have a more migratory phenotype.

Both the immunostaining and Western Blot results demonstrate that silencing the Nck genes can reduce the progression of EndMT in HUVEC cells.

CHAPTER IV

CONCLUSIONS

Atherosclerosis and many cancers promote angiogenesis which results in leaky, poorly perfused vasculature, that decreases blood vessel integrity and promotes rapid proliferation and metastasis for tumor (Chen et al., 2015a). The endothelial to mesenchymal transition is a major step in promotion of abnormal tumor vasculature, as it disrupts the cells that line blood vessels. The vascular endothelial cells under certain stressful environment with TGF-β2 signaling molecule can undergo a switch in phenotype from endothelial to a more mesenchymal-like morphology (Cooley et al., 2014). In this study, the induction of TGF-β2 to HUVECs resulted in a downregulation of VE-Cadherin thereby decreasing cell-to-cell junctions. As the endothelial cells morph into fibroblast-like cells, they downregulate their VE-Cadherin expression, and express more stress fibers (f-actin).

In this research study, the role played by the Nck family of adaptor proteins, known to facilitate cytoskeletal remodeling, was better defined. A baseline was established; in the presence of TGF-β2 signaling molecule there was a shift in HUVEC phenotype. Results following this establishment indicate that Nck seems to attenuate this shift in phenotype when compared to the control. I plan to repeat this experimental design in order to collect more data to support this hypothesis.

These findings are significant because development of angiogenesis drugs that target the TGF-β2 pathway, or cause reversal of TGF-β2 induced changes can reduce abnormal development of the vascular system, increase the profusion of cancer drugs to the cancer cells, and decrease the chances of malignancy.

REFERENCES

Bordeleau, F., J.P. Califano, Y.L. Negron Abril, B.N. Mason, D.J. LaValley, S.J. Shin, R.S. Weiss, and C.A. Reinhart-King. 2015. Tissue stiffness regulates serine/arginine-rich protein-mediated splicing of the extra domain B-fibronectin isoform in tumors. Proceedings of the National Academy of Sciences of the United States of America. 112:8314-8319.

Baumgartner, W., G.J. Schutz, J. Wiegand, N. Golenhofen, and D. Drenckhahn. 2003. Cadherin function probed by laser tweezer and single molecule fluorescence in vascular endothelial cells. J Cell Sci. 116:1001-1011.

Climent, M., M. Quintavalle, M. Miragoli, J. Chen, G. Condorelli, and L. Elia. 2015. TGFbeta Triggers miR-143/145 Transfer From Smooth Muscle Cells to Endothelial Cells, Thereby Modulating Vessel Stabilization. *Circulation research*. 116:1753-1764.

Clouthier, D.L., C.N. Harris, R.A. Harris, C.E. Martin, M.C. Puri, and N. Jones. 2015. Requisite role for Nck adaptors in cardiovascular development, endothelial-to-mesenchymal transition, and directed cell migration. Mol Cell Biol. 35:1573-1587.

Cooley, B.C., J. Nevado, J. Mellad, D. Yang, C. St Hilaire, A. Negro, F. Fang, G. Chen, H. San, A.D. Walts, R.L. Schwartzbeck, B. Taylor, J.D. Lanzer, A. Wragg, A. Elagha, L.E. Beltran, C. Berry, R. Feil, R. Virmani, E. Ladich, J.C. Kovacic, and M. Boehm. 2014. TGF-beta signaling mediates endothelial-to-mesenchymal transition (EndMT) during vein graft remodeling. Science translational medicine. 6:227ra234.

Erasmus, J.C., S. Bruche, L. Pizarro, N. Maimari, T. Pogglioli, C. Tomlinson, J. Lees, I. Zalivina, A. Wheeler, A. Alberts, A. Russo, and V.M. Braga. 2016. Defining functional interactions during biogenesis of epithelial junctions. Nature communications. 7:13542.

Jung, K., T. Heishi, O.F. Khan, P.S. Kowalski, J. Incio, N.N. Rahbari, E. Chung, J.W. Clark, C.G. Willett, A.D. Luster, S.H. Yun, R. Langer, D.G. Anderson, T.P. Padera, R.K. Jain, and D. Fukumura. 2017. Ly6Clo monocytes drive immunosuppression and confer resistance to anti-VEGFR2 cancer therapy. The Journal of clinical investigation. 127:3039-3051.

Liu, J., S. Liao, B. Diop-Frimpong, W. Chen, S. Goel, K. Naxerova, M. Ancukiewicz, Y. Boucher, R.K. Jain, and L. Xu. 2012. TGF-beta blockade improves the distribution and efficacy of therapeutics in breast carcinoma by normalizing the tumor stroma. *Proceedings of the National Academy of Sciences of the United States of America*. 109:16618-16623.

Momiyama Y., Adachi H., Fairweather D., Ishizaka N., Saita E. (2014) Inflammation, Atherosclerosis and Coronary Artery Disease. Clin. Med. Insights Cardiol. 8(Suppl. 3):67–70.

Miroshnikova, Y.A., J.K. Mouw, J.M. Barnes, M.W. Pickup, J.N. Lakins, Y. Kim, K. Lobo, A.I. Persson, G.F. Reis, T.R. McKnight, E.C. Holland, J.J. Phillips, and V.M. Weaver. 2016. Tissue mechanics promote IDH1-dependent HIF1alpha-tenascin C feedback to regulate glioblastoma aggression. Nat Cell Biol. 18:1336-1345.

Pils S, Kopp K, Peterson L, Delgado Tascón J, Nyffenegger-Jann NJ, Hauck CR. (2012) The adaptor molecule Nck localizes the WAVE complex to promote actin polymerization during CEACAM3-mediated phagocytosis of bacteria. PLoS One 7:e32808.10.1371

Rigamonti, N., E. Kadioglu, I. Keklikoglou, C. Wyser Rmili, C.C. Leow, and M. De Palma. 2014. Role of angiopoietin-2 in adaptive tumor resistance to VEGF signaling blockade. Cell reports. 8:696- 706.

Welch-Reardon, K.M., S.M. Ehsan, K. Wang, N. Wu, A.C. Newman, M. Romero-Lopez, A.H. Fong, S.C. George, R.A. Edwards, and C.C.W. Hughes. 2014. Angiogenic sprouting is regulated by endothelial cell expression of Slug. Journal of Cell Science. 127:2017-2028.

Zeisberg, E.M., S. Potenta, L. Xie, M. Zeisberg, and R. Kalluri. 2007a. Discovery of endothelial to mesenchymal transition as a source for carcinoma-associated fibroblasts. Cancer research. 67:10123-10128.

APPENDIX

REAGENTS USED FOR THE EXPERIMENTS

Table 4. Reagents used to culture and harvest cells

Process	Reagent		Vendor	Catalogue number
Preparation for FN-coated coverslips	18 mm round coverslips		VWR- Vista Vision	16004 - 300
	Fibronectin (100 μg/μL)		Millipore	341635
Cell Culture and Passing	EGM2 Bullet kit (EBM2 Basal Media + growth factors)		Lonza	CC-3162
	HUVEC		LN2	R4B2
	Trypsin/EDTA (0.25mg/mL)		Lonza	CC5012
	Phosphate Buffered Saline (PBS)		Gibco - Invitrogen	10010-013
	3% FBS in PBS (Phosphate Buffered Saline)		FBS – Nalgene	CC-4101A
Induction of EndoMT via TGF-β2 stimulation	10 ng /mL TGF-β2 Stock 20 ng/μL		Gibco - Invitrogen	PH 69114
	Endothelial starvation media w/ 0.2 % FBS	EBM2 Basal Media	Lonza	CC-3162
		FBS	Lonza	CC-4101A

Table 5. Reagents used for immunofluorescence staining

Step	Materials: Mixed compound / stock solution		Stock Solution Company	Catalog Number
Fixing	4% Paraformaldehyde in DPBS	16 % Paraformaldehyde	Electron Microscopy Sciences	Cat # 15710
		PBS 1X	Gibco - Invitrogen	10010 - 031
Blocking	0.2% Triton X-100 in CB	Triton™ X-100	VWR International	VW 3929-2
	2% BSA in CB	BSA	Fisher Bio Reagents	CAS 9048-46-8
Primary Dilution	Whatman™ Chromatography Paper		NuPAGE®	3030-6188
	CD31		Abcam	ab 28364
	SM22-α		Abcam	ab 14106
	VE-Cadherin		Santa Cruz	sc -9989
	Vimentin		Santa Cruz	sc - 6260
	2% BSA in CB	BSA	Fisher Bio Reagents	CAS 9048-46-8
Washing	2% BSA and 0.2% Tween® 20 in CB		Fisher Scientific	CAS 9005-64-5
Secondary Dilution	Alexa Fluor® 488 Goat Anti-Rabbit IgG		Life Technologies	A-11029
	Whatman™ Chromatography Paper		NuPAGE®	3030-6188
	Texas Red®-X Phalloidin		Life Technologies	T7471
	NucBlue® Live ReadyProbes® Reagent		Life Technologies	R37605
	2% BSA in CB	BSA	Fisher Bio Reagents	CAS 9048-46-8
Mounting	Prolong® Gold Antifade Mountant		Life Technologies	P36934

Part 1: Immunofluorescence solution recipe

Cytoskeletal Buffer

1. Add compounds into a 500 mL flask
   - 150 mM NaCl
   - 10 mM MES
   - 5 mM MgCl2
   - 5 mM EGTA 5 mM glucose
   - 400 mL ddH2O

2. Adjust pH the buffer to 6.1 with NaOH.

Table 6. Primary antibodies dilutions for IF

Primary Antibody	Blocking Solution	Antibody Concentration
CD31	BSA in CB	1:500
SM22-α	BSA in CB	1:500
VE-Cadherin	BSA in CB	1:750
Vimentin	BSA in CB	1:750

Table 7. Secondary antibodies dilutions for IF

Secondary Antibody	Primary Antibodies Targeted	Secondary Antibody Concentration
Goat anti-Mouse IgG 488	VE-Cad	1:500
	Vimentin	
Goat anti-Rabbit IgG 647	CD31	1:500
	SM22-α	
Texas Red®-X Phalloidin	F-actin	1:200
NucBlue® Live ReadyProbes® Reagent	Nucleus	2 drops /mL